J|A|C|S
ARTICLES
Published on Web 11/17/2006

What Factors Influence the Ratio of C−H Hydroxylation versus C=C Epoxidation by a Nonheme Cytochrome P450 Biomimetic?

Sam P. de Visser

Contribution from the Manchester Interdisciplinary Biocenter and the School of Chemical Engineering and Analytical Science, The University of Manchester, 131 Princess Street, Manchester M1 7DN, United Kingdom

Received July 26, 2006; E-mail: sam.devisser@manchester.ac.uk

Abstract: Density functional calculations on a nonheme biomimetic (Fe=O(TMCS)$^+$) have been performed and its catalytic properties versus propene investigated. Our studies show that this catalyst is able to chemoselectively hydroxylate C−H bonds *even in the presence of C=C double bonds*. This phenomenon has been analyzed and found to occur due to Pauli repusions between protons on the TMCS ligand with protons attached to the approaching substrate. The geometries of the rate determining transition states indicate that the steric hindrance is larger in the epoxidation transition states than in the hydroxylation ones with much shorter distances; hence the hydroxylation pathway is favored over the epoxidation. Although, the reactant experiences close lying triplet and quintet spin states, the dominant reaction mechanism takes place on the quintet spin state surface; i.e., Fe=O(TMCS)$^+$ reacts via single-state reactivity. Our calculations show that this spin state selectivity is the result of geometric orientation of the transition state structures, whereby the triplet ones are destabilized by electrostatic repulsions between the substrate and the ligand while the quintet spin transition states are aligned along the ideal axis. The reactivity patterns and geometries are compared with oxoiron species of dioxygenase and monoxygenase enzymes. Thus, Fe=O(TMCS)$^+$ shows some similarities with P450 enzyme reactivity: it chemoselectively hydroxylates C−H bonds even in the presence of a C=C double bond and therefore is an acceptable P450 biomimetic. However, the absolute barriers of substrate oxidation by Fe=O(TMCS)$^+$ are higher than the ones obtained with heme enzymes, but the chemoselectivity is lesser affected by external perturbations such as hydrogen bonding of a methanol molecule toward the thiolate sulfur or a dielectric constant. This is the first oxoiron complex whereby we calculated a chemoselective hydroxylation over epoxidation in the gas phase.

Introduction

Biomimetics are synthetic inorganic catalysts of which the structure and chemical features are based upon biological templates.[1] These catalysts are being generated for commercial as well as environmental purposes and have been shown to be very versatile and efficient. One of the challenging tasks in biocatalysis is the generation of systems that can mimic the catalytic properties of enzymes. For various reasons the synthesis of analogues of the active site of the cytochromes P450 (P450) have proved to be particularly difficult, but recent models have given promising prospects.[1b,2,3]

The P450s are heme enzymes that utilize molecular oxygen and are involved in the metabolism of drugs and the detoxification of compounds in biosystems.[4] The catalytic center contains a central iron atom that is bound to the peptide backbone via a thiolate linkage of a cysteinate residue.[5] This is a common feature that this class of enzymes shares with other enzymes such as chloroperoxidase (CPO)[6] and nitric oxide synthase (NOS).[7] Despite many experimental efforts to trap and characterize the active species of P450 (Compound I, CpdI) it still remains elusive, but it is believed to be in the oxoiron form.[8] Extensive studies on synthetic oxoiron porphyrin systems and supporting theoretical modeling into the nature of CpdI identified the most likely candidate to be the oxoiron(IV) species.[4,9] For some enzymes, such as CPO and horseradish peroxidase (HRP), the oxoiron(IV) species has been trapped and characterized experimentally.[6,10]

(1) (a) Costas, M.; Mehn, M. P.; Jensen, M. P.; Que, L., Jr. *Chem. Rev.* **2004**, *104*, 939−986. (b) Woggon, W.-D. *Acc. Chem. Res.* **2005**, *38*, 127−136. (c) Shan, X.; Que, L., Jr. *J. Inorg. Biochem.* **2006**, *100*, 421−433.
(2) Fiedler, A. T.; Halfen, H. L.; Halfen, J. A.; Brunold, T. C. *J. Am. Chem. Soc.* **2005**, *127*, 1675−1689.
(3) Bukowski, M. R.; Koehntop, K. D.; Stubna, A.; Bominaar, E. L.; Halfen, J. A.; Münck, E.; Nam, W.; Que, L., Jr. *Science* **2005**, *310*, 1000−1002.
(4) (a) Sono, M.; Roach, M. P.; Coulter, E. D.; Dawson, J. H. *Chem. Rev.* **1996**, *96*, 2841−2887. (b) Groves, J. T. *Proc. Natl. Acad. Sci. U.S.A.* **2003**, *100*, 3569−3574. (c) Ortiz de Montellano, P. R., Ed. *Cytochrome P450: Structure, Mechanism and Biochemistry*, 3rd ed.; Kluwer Academic/Plenum Publishers: New York, 2004.
(5) (a) Poulos, T. L.; Finzel, B. C.; Howard, A. J. *Biochemistry* **1986**, *25*, 5314−5322. (b) Schlichting, I.; Berendzen, J.; Chu, K.; Stock, A. M.; Maves, S. A.; Benson, D. E.; Sweet, R. M.; Ringe, D.; Petsko, G. A.; Sligar, S. G. *Science* **2000**, *287*, 1615−1622.
(6) Green, M. T.; Dawson, J. H.; Gray, H. B. *Science* **2004**, *304*, 1653−1656.
(7) (a) Groves, J. T.; Wang, C. C. *Curr. Opin. Chem. Biol.* **2000**, *4*, 687−695. (b) Stuehr, D. J.; Santolini, J.; Wang, Z.-Q.; Wei, C.-C.; Adak, S. *J. Biol. Chem.* **2004**, *279*, 36167−16170.
(8) Denisov, I. G.; Makris, T. M.; Sligar, S. G.; Schlichting, I. *Chem. Rev.* **2005**, *105*, 2253−2277.

Some biomimetics can catalyze substrates with higher turnover numbers and greater efficiency than enzymes and have longer lifetimes.[1a] In particular, the oxoiron(IV) species of several nonheme biomimetics have been synthesized and characterized, and detailed reactivity patterns were studied versus a range of substrates. Recently a nonheme oxoiron complex with a pentadentate ligand labeled N4Py (N4Py = *N*,*N*-bis(2-pyridylmethyl)-bis(2-pyridyl)methylamine) was characterized spectroscopically and its catalytic properties were studied versus a range of typical reagents.[11] Thus, oxoiron(N4Py)$^{2+}$ was even found to be able to catalyze hydroxylation reactions of strong C—H bonds such as, for instance, those that appear in cyclohexane.[11a] Another nonheme oxoiron complex that has been studied extensively is the Fe═O(TMC)(NCCH$_3$)$^{2+}$ model (TMC = 1,4,8,11-tetramethyl-1,4,8,11-tetraazacyclotetradecane) and a high-resolution crystal structure was determined.[12] This oxoiron catalyst was found to react via sulfoxidation with thioanisole quantitatively at 35 °C.[13] Studies into the possibility of alternative oxidants in the reaction process revealed that the precursor of the oxoiron complex in the catalytic cycle, i.e., the hydroperoxoiron complex, is a sluggish oxidant toward thioanisole oxidation and is not able to compete with the oxoiron complex.[13] The work, therefore, identified the nature of the oxidant and ruled out several possible alternative oxidants in the reaction process. Further studies on the Fe═O(TMC)$^{2+}$ complex revealed a considerable axial ligand effect on the spectroscopic and catalytic properties of the system.[14] Three different ligands were investigated (NCCH$_3$, NCS$^-$, and N$_3^-$), and the second-order rate constants for oxidation of PPh$_3$ showed differences of up to a factor of 30. Thus, nonheme oxoiron complexes much like oxoiron heme complexes experience a strong axial ligand effect that can influence the charge distribution on the oxoiron unit and consequently its reactivity patterns. In heme chemistry it was shown that the axial ligand trans to the oxo group influences the electronic properties of the transition metal and thereby the catalytic properties of the enzyme.[15] Thus, the push effect of the thiolate ligand was identified as one of the key reasons why the P450s show dominant hydroxylation reactions.[16]

In nonheme systems the axial ligand also affects the reactivity patterns strongly.[14] The effect of a thiolate ligand on the catalytic properties of nonheme oxoiron complexes was studied using a biomimetic system containing a pentadentate ligand that is the monoanion of 1-mercaptoethyl-4,8,11-trimethyl-1,4,8,11-tetraazacyclotetradecane (TMCS), Scheme 1.[2,3] It was shown that this system can mimic P450 reactivity as a hydrogen abstraction agent. Scheme 1 shows the chemical structure of the two catalysts as compared in this work. At first glance, the two structures seem quite distinct, but in fact the iron atom is bound to the same set of atoms, namely an oxo group in the distal position, a sulfur atom of a thiolate group in the axial position, and four nitrogen atoms perpendicular to this O—Fe—S axis. However, there is an essential electronic difference, namely the oxoiron heme model has one oxidation equivalent located on the heme, while in the nonheme TMCS model oxidation of the ligand is much harder. As we shall show here, this affects the overall spin state of the system and consequently its reactivity pattern. Thus, in order to find out whether Fe═O(TMCS)$^+$ indeed preferentially reacts via hydroxylation rather than epoxidation and the chemical reasons behind this, we have pursued a density functional theoretic study into the chemoselectivity of C—H hydroxylation versus C═C epoxidation by Fe═O(TMCS)$^+$. In this work we will address the issues that influence the chemoselectivity of hydroxylation versus epoxidation and explain the factors that determine the product ratios. In the past, we extensively studied the monoxygenation activity of oxoiron complexes versus propene since this is the smallest chemical system where competitive hydroxylation and epoxidation mechanisms are possible.[17,18] In all these cases in the gas phase, the epoxidation reaction was favored over the hydroxylation and external perturbations had to be applied to

Scheme 1. Molecular Structures of (a) Fe═O(TMCS)$^+$ and (b) CpdI of Cytochrome P450 as Studied in This Work

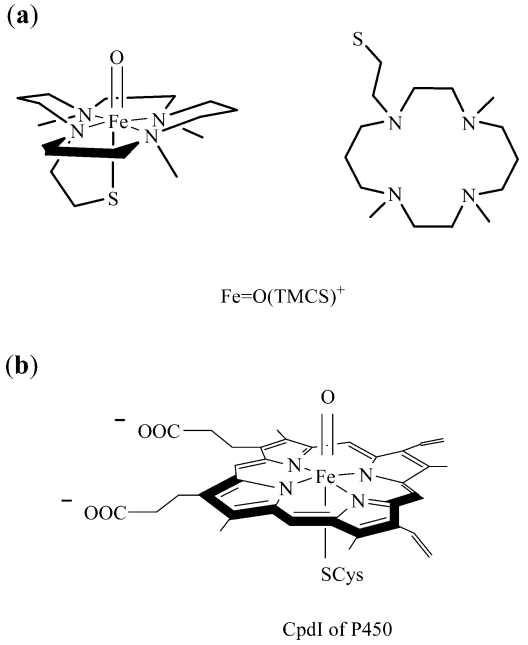

(9) (a) Green, M. T. *J. Am. Chem. Soc.* **1998**, *120*, 10772−10773. (b) Harris, D. L. *Curr. Opin. Chem. Biol.* **2001**, *5*, 724−735. (c) Meunier, B.; de Visser, S. P.; Shaik, S. *Chem. Rev.* **2004**, *104*, 3947−3980. (d) Kumar, D.; Hirao, H.; de Visser, S. P.; Zheng, J.; Wang, D.; Thiel, W.; Shaik, S. *J. Phys. Chem. B* **2005**, *109*, 19946−19951.

(10) Berglund, G. I.; Carlsson, G. H.; Smith, A. T.; Szöke, H.; Henriksen, A.; Hajdu, J. *Nature* **2002**, *417*, 463−468.

(11) (a) Kaizer, J.; Klinker, E. J.; Oh, N. Y.; Rohde, J.-U.; Song, W. J.; Stubna, A.; Kim, J.; Münck, E.; Nam, W.; Que, L., Jr. *J. Am. Chem. Soc.* **2004**, *126*, 472−473. (b) Klinker, E. J.; Kaizer, J.; Brennessel, W. W.; Woodrum, N. L.; Cramer, C. J.; Que, L., Jr. *Angew. Chem., Int. Ed.* **2005**, *44*, 3690−3694.

(12) Rohde, J.-U.; In, J.-H.; Lim, M. H.; Brennessel, W. W.; Bukowski, M. R.; Stubna, A.; Münck, E.; Nam, W.; Que, L., Jr. *Science* **2003**, *299*, 1037−1039.

(13) Park, M. J.; Lee, J.; Kim, J.; Nam, W. *J. Am. Chem. Soc.* **2006**, *128*, 2630−2634.

(14) Sastri, C. V.; Park, M. J.; Ohta, T.; Jackson, T. A.; Stubna, A.; Seo, M. S.; Lee, J.; Kim, J.; Kizagawa, T.; Münck, E.; Que, L., Jr.; Nam, W. *J. Am. Chem. Soc*. **2005**, *127*, 12494−12495.

(15) (a) Gross, Z.; Nimri, S. *Inorg. Chem.* **1994**, *33*, 1731−1732. (b) Czarnecki, K.; Nimri, S.; Gross, Z.; Proniewicz, L. M.; Kincaid, J. R. *J. Am. Chem. Soc.* **1996**, *118*, 2929−2935.

(16) (a) Dawson, J. H.; Holm, R. H.; Trudell, J. R.; Barth, G.; Linder, R. E.; Bunnenberg, E.; Djerassi, C.; Tang, S. C. *J. Am. Chem. Soc.* **1976**, *98*, 3707−3709. (b) Poulos, T. L. *J. Biol. Inorg. Chem.* **1996**, *1*, 356−359. (c) Shaik, S.; Kumar, D.; de Visser, S. P.; Altun, A.; Thiel, W. *Chem. Rev.* **2005**, *105*, 2279−2328.

(17) (a) de Visser, S. P. *Angew. Chem., Int. Ed*. **2006**, *45*, 1790−1793; *Angew. Chem.* **2006**, *118*, 1822−1825. (b) de Visser, S. P. *J. Am. Chem. Soc.* **2006**, *128*, 9813−9824.

(18) (a) de Visser, S. P.; Ogliaro, F.; Sharma, P. K.; Shaik, S. *Angew. Chem., Int. Ed.* **2002**, *41*, 1947−1951. (b) de Visser, S. P.; Ogliaro, F.; Sharma, P. K.; Shaik, S. *J. Am. Chem. Soc.* **2002**, *124*, 11809−11826. (c) Kumar, D.; de Visser, S. P.; Sharma, P. K.; Derat, E.; Shaik, S. *J. Biol. Inorg. Chem.* **2005**, *10*, 181−189. (d) de Visser, S. P. *J. Biol. Inorg. Chem.* **2006**, *11*, 168−178.

change the chemoselectivity. So what makes Fe═O(TMCS)$^+$ such a special catalyst that it can catalyze alkyl hydroxylations even in the presence of a C═C double bond? This tantalizing question will be addressed in the current paper.

Methods

We use commonly accepted and applied methods which we will briefly summarize here.[19] The calculations were performed using the Jaguar 5.5 program package[20] and utilized the UB3LYP hybrid density functional method.[21] We employed a double-ζ quality LACVP basis set on iron in combination with a 6-31G basis set on the rest of the atoms[22] to optimize the geometries. Improvement of the energetics was achieved with a subsequent single-point calculation using the triple-ζ quality LACV3P+* basis set on iron in combination with a 6-311+G* basis set on the rest of the atoms.[22] The nature of the critical points was verified with an analytical frequency calculation in Gaussian-03.[23] All local minima had real frequencies only, and the transition states had one imaginary frequency for the correct mode. In order to study the chemoselectivity between C—H hydroxylation and C═C epoxidation we used propene as a substrate since this is the smallest model in which competitive alkyl hydroxylation and C═C double bond epoxidation mechanisms can be studied.[17,18] Moreover, it enables us to make a direct comparison of the catalytic properties of Fe═O(TMCS)$^+$ with oxoiron systems in P450 and taurine/α-ketoglutarate dioxygenase (TauD) models.[17,18]

The effect of the environment on the ordering and relative energies of the transition states was tested by the addition of a dielectric constant of either $\epsilon = 5.7$ or 10.65. These calculations used the self-consistent reaction field (SCRF) model as implemented in Jaguar with a probe radius of 2.72 and 2.51 Å, respectively.

We also calculated the effect of hydrogen bonding interactions pointing toward the thiolate ligand, since previous work showed that these interactions can influence the electronic configuration of thiolate ligated oxoiron systems considerably.[24] Initially we added one or two hydrogen-bonded methanol molecules toward the sulfur atom of TMCS at a 2.3 Å distance but later also performed full geometry optimizations for the reactants and rate determining transition states with one hydrogen-bonded methanol molecule.

Results and Discussion

Electronic Properties of ^{1,3,5}Fe═O(TMCS)$^+$. The high-lying occupied and low-lying virtual orbitals of Fe═O(TMCS)$^+$ are dominated by the metal 3d orbitals (Figure 1), which split into the usual t_{2g}—e_g set of orbitals. The e_g subset corresponds to the two σ^* antibonding orbitals: one along the O—Fe—S axis (σ^*_{z2}) and the other in the plane of the four nitrogen atoms (σ^*_{xy}). These orbitals look similar in shape for the singlet, triplet, and quintet spin states and compare well with the ones obtained for the oxoiron(IV) species of P450 models.[9a,25] By contrast, the oxoiron(IV) species of TauD is surrounded by weak ligands (two imidazole groups of histidine residues and two carboxylic acid groups) that do not interact much with the metal.[17] As a result, the $\sigma^*_{z^2}$ and σ^*_{xy} orbitals of the oxoiron(IV) species in

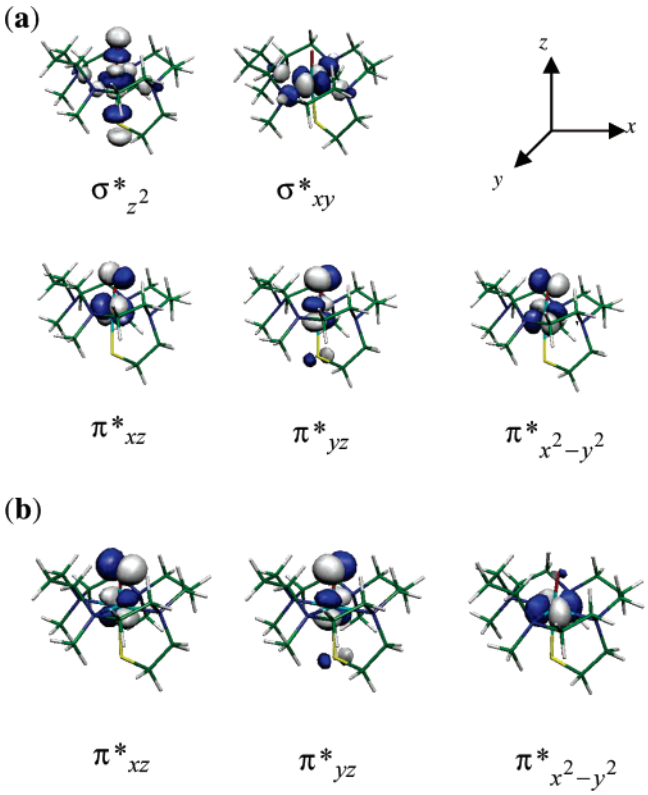

Figure 1. High-lying occupied and low-lying virtual orbitals of Fe═O(TMCS)$^+$ drawn with Molekel.[26] (a) Molecular orbitals of ^{5}Fe═O(TMCS)$^+$. (b) π^* orbitals of ^{3,1}Fe═O(TMCS)$^+$.

TauD have much less antibonding character and are lower in energy. The three t_{2g} orbitals in Fe═O(TMCS)$^+$ are π^*-type and represent the antibonding interactions along the Fe—O bond. Figure 1a shows the π^* and σ^* set of orbitals of ^{5}Fe═O(TMCS)$^+$, whereas Figure 1b displays the π^* ones of ^{1,3}Fe═O(TMCS)$^+$ drawn using the Molekel program package.[26] The π^*_{yz} orbital in all three spin states is aligned along the *z*-axis and is antibonding with the oxygen as well as the sulfur atoms. The π^*_{xz} and $\pi^*_{x^2-y^2}$ orbitals in the quintet spin state mix in such a way that the metal 3d lobes are tilted with respect to the plane through the four nitrogen atoms (the *xy*-plane). These orbitals match the ones obtained for the oxoiron species of TauD excellently.[17] In contrast to this, in the singlet and triplet spin states there is no mixing between the π^*_{xz} and $\pi^*_{x^2-y^2}$ orbitals, and as a result the π^*_{xz} orbital is in the *xz*-plane along the O—Fe—S axis, while the $\pi^*_{x^2-y^2}$ orbital is in the plane through the four nitrogen atoms. The latter orbital is prevented from orbital overlap with neighboring atoms and is reduced to a nonbonding orbital. The same situation occurs in oxoiron(IV) heme systems whereby the plane of the heme creates a nonbonding $3d_{x^2-y^2}$ (δ) orbital. Due to significant stabilization of this $3d_{x^2-y^2}$ orbital in heme systems the overall spin multiplicity of the oxoiron(IV) heme system is generally lower than that in analogous nonheme systems. Hence, the ground state of oxoiron(IV) heme systems has a doubly occupied $\pi^*_{x^2-y^2}$ orbital and triplet coupled π^*_{xz} and π^*_{yz} electrons. In nonheme models such as Fe═O(TMCS)$^+$ the $\pi^*_{x^2-y^2}$ orbital is much higher lying, and as a result the system can exist in an overall quintet spin state with occupation $\pi^*_{x^2-y^2}{}^1\,\pi^*_{xz}{}^1\,\pi^*_{yz}{}^1\,\sigma^*_{xy}{}^1$ or in an overall triplet or singlet spin state with occupation $\pi^*_{x^2-y^2}{}^2\,\pi^*_{xz}{}^1\,\pi^*_{yz}{}^1$ (Scheme

(19) (a) de Visser, S. P.; Kumar, D.; Cohen, S.; Shacham, R.; Shaik, S. *J. Am. Chem. Soc.* **2004**, *126*, 8362−8363. (b) de Visser, S. P. *J. Phys. Chem. A* **2005**, *109*, 11050−11057.
(20) *Jaguar 5.5*; Schrödinger, LLC: Portland, OR, 2003.
(21) (a) Becke, A. D. *J. Chem. Phys.* **1993**, *98*, 5648−5652. (b) Lee, C.; Yang, W.; Parr, R. G. *Phys. Rev. B* **1988**, *37*, 785−789.
(22) Hay, P. J.; Wadt, W. R. *J. Chem. Phys.* **1985**, *82*, 299−310.
(23) Frisch, M. J., et al. *Gaussian-03*, revision C.01. See Supporting Information.
(24) (a) Ogliaro, F.; Cohen, S.; de Visser, S. P.; Shaik, S. *J. Am. Chem. Soc.* **2000**, *122*, 12892−12893. (b) de Visser, S. P.; Shaik, S. *J. Am. Chem. Soc.* **2003**, *125*, 7413−7424.
(25) (a) Ogliaro, F.; de Visser, S. P.; Groves, J. T.; Shaik, S. *Angew. Chem., Int. Ed.* **2001**, *40*, 2874−2878. (b) de Visser, S. P.; Shaik, S.; Sharma, P. K.; Kumar, D.; Thiel, W. *J. Am. Chem. Soc.* **2003**, *125*, 15779−15788.
(26) Molekel, Version 4.3.win32 by Portmann, S., CSCS/ETHZ, 2002.

Scheme 2. Orbital Occupation of ^{5,3}Fe═O(TMCS)$^+$ (^{5,3}**1**)

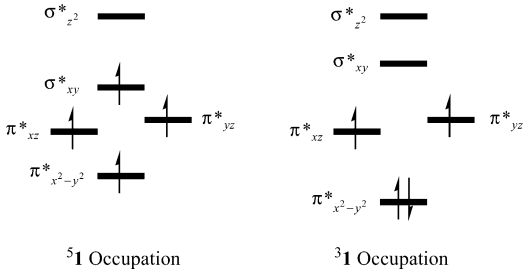

2). The ordering of the quintet, triplet, and singlet spin states is, therefore, dependent on the exchange stabilization of the 3d metal orbitals and the relative energy of the $\pi^*_{x^2-y^2}$ and σ^*_{xy} orbitals. A large energy gap between $\pi^*_{x^2-y^2}$ and σ^*_{xy}, as is the case in heme enzymes, will stabilize a situation with $\pi^*_{x^2-y^2}{}^2$ $\pi^*_{xz}{}^1$ $\pi^*_{yz}{}^1$ occupation. On the other hand, if the exchange stabilization of the four 3d orbitals exceeds the energy difference between the $\pi^*_{x^2-y^2}$ and σ^*_{xy} orbitals, a high-spin situation will be favored. This situation occurs in the pentacoordinated oxoiron active species of TauD. In summary, the molecular orbitals of ^{3,1}Fe═O(TMCS)$^+$ show similarities with oxoiron(IV) heme systems, whereas ^{5}Fe═O(TMCS)$^+$ has orbitals matching the oxoiron(IV) nonheme systems as obtained in TauD. Actually, three valence orbitals, i.e., the π^*_{yz}, σ^*_{xy}, and $\sigma^*_{z^2}$, are analogously in all spin states and resemble heme-type oxoiron(IV) orbitals. However, the other two valence orbitals, i.e., $\pi^*_{x^2-y^2}$ and π^*_{xz}, determine the actual character of the catalyst whether it has overall heme or nonheme orbital equivalents. This will have a serious impact on the nature of the electronic ground state and the reactivity pattern of Fe═O(TMCS)$^+$. In TauD the quintet spin state was the ground state with the triplet spin state 15.8 kcal mol^{-1} higher.[17]

Structure and Spin-State Ordering of Fe═O(TMCS)$^+$. Figure 2 shows the optimized geometries and relative energies of ^{5,3,1}Fe═O(TMCS)$^+$ (^{5,3,1}**1**). We find a quintet spin ground state with the triplet and singlet states higher by 4.4 and 13.4 kcal mol^{-1}. Magnetic susceptibility studies on Fe^{II}(TMCS)$^+$ structures identified a quintet spin ground state at room temperature in agreement with what we obtain here.[2] As reasoned above we indeed find a small quintet−triplet energy gap that is considerably smaller than the one found in TauD due to more antibonding character of the π^*_{yz} and σ^*_{xy} orbitals. Since, the quintet spin state in TauD is well separated from the singlet and triplet spin states, the oxoiron(IV) species reacts via single-state reactivity (SSR) with substrates on a dominant quintet spin state surface,[17b] whereas Fe═O(TMCS)$^+$ is expected to react via two-state reactivity (TSR) patterns on competing triplet and quintet spin state surfaces. However, as will be shown later in this work, the reaction barriers on the triplet surface are much higher than the ones obtained on the quintet spin state surface resulting in SSR patterns for Fe═O(TMCS)$^+$.

Also shown in Figure 2 are the group spin densities (ρ) of ^{5,3,1}Fe═O(TMCS)$^+$. Single occupation of the $\pi^*_{x^2-y^2}$, π^*_{xz}, π^*_{yz}, and σ^*_{xy} orbitals leads to a spin density of 3.90 on the FeO unit, while the rest is on the four nitrogen atoms. Note that in the triplet spin state the spin density of the FeO unit is strongly polarized toward the iron atom (ρ_{Fe} = 1.33 and ρ_O = 0.76), which is in contrast to heme enzymes, whereby generally equal spin densities on the iron and oxygen atoms are found in CpdI.[25]

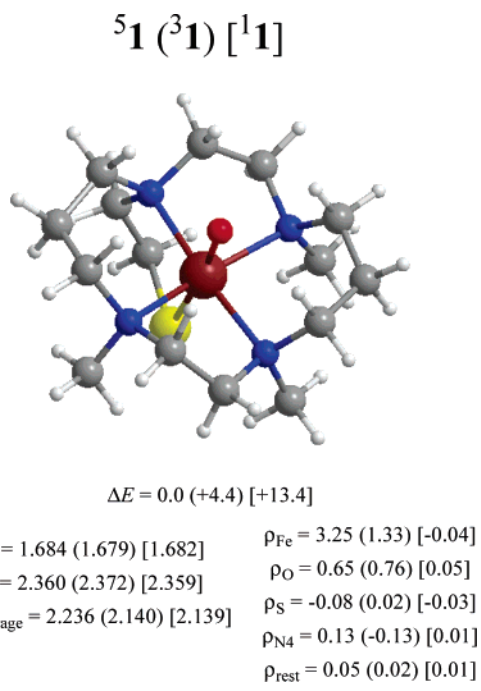

Figure 2. Optimized geometries (with bond lengths in angstroms), relative energies (ΔE relative to ^{5}**1** in kcal mol^{-1}), and group spin densities (ρ) of ^{5,3,1}**1** as calculated with UB3LYP/LACVP in Jaguar. Results in parentheses are for the triplet spin state, and data in square brackets refer to the singlet spin state. Relative energies and group spin densities were taken from the LACV3P+* calculations.

Since, the singlet, triplet, and quintet spin states of Fe═O(TMCS)$^+$ only differ in the occupation of the $\pi^*_{x^2-y^2}$ and σ^*_{xy} orbitals, the differences in geometry are mainly in the *xy*-plane of symmetry, i.e., in the plane through the four nitrogen atoms. Indeed, the Fe—O and Fe—S distances are similar, and our optimized geometries predict Fe—O distances of 1.684 (1.679) [1.682] Å and Fe—S distances of 2.360 (2.372) [2.359] Å for ^{5}**1** (^{3}**1**) [^{1}**1**]. These distances match the experimentally obtained values of 1.70 (Fe—O) and 2.33 (Fe—S) Å excellently.[3] Our optimized geometries of ^{3,5}**1** are in good agreement with earlier DFT studies.[3,27]

Note that a free SH$^-$ anion as used in P450 models (Fe═O(Por$^{+\bullet}$)SH) gives a much longer Fe—S bond of 2.6 Å[25] than the constraint system studied here. This is mainly due to the fact that the thiolate orbitals in P450 mix with a singly occupied heme orbital (a_{2u}), and as a result there is a significant amount of spin density (and radical character) on the thiolate ligand of Fe═O(Por$^{+\bullet}$)SH that weakens the Fe—S bond,[9,25] while in ^{5,3,1}Fe═O(TMCS)$^+$ there is little or no radical character on the sulfur atom and the rest of the TMCS ligand. An additional difference between the two models is that the cavity of the ligand plane is much larger in TMCS with average Fe—N distances of 2.236 (2.140) Å for ^{5,3}**1**, while the average distance is only 2.017 Å in Fe═O(Por$^{+\bullet}$)SH.[25] The large Fe—N distances in the quintet spin state are the result of single occupation of the antibonding σ^*_{xy} orbital that weakens the Fe—N distances. The triplet and singlet optimized geometries are essentially the same due to identical orbital occupation.

Epoxidation by Fe═O(TMCS)$^+$. In order to test the catalytic properties of Fe═O(TMCS)$^+$ (^{1,3,5}**1**) and in particular the

(27) Conradie, J.; Wasbotten, I.; Ghosh, A. *J. Inorg. Biochem.* **2006**, *100*, 502−506.

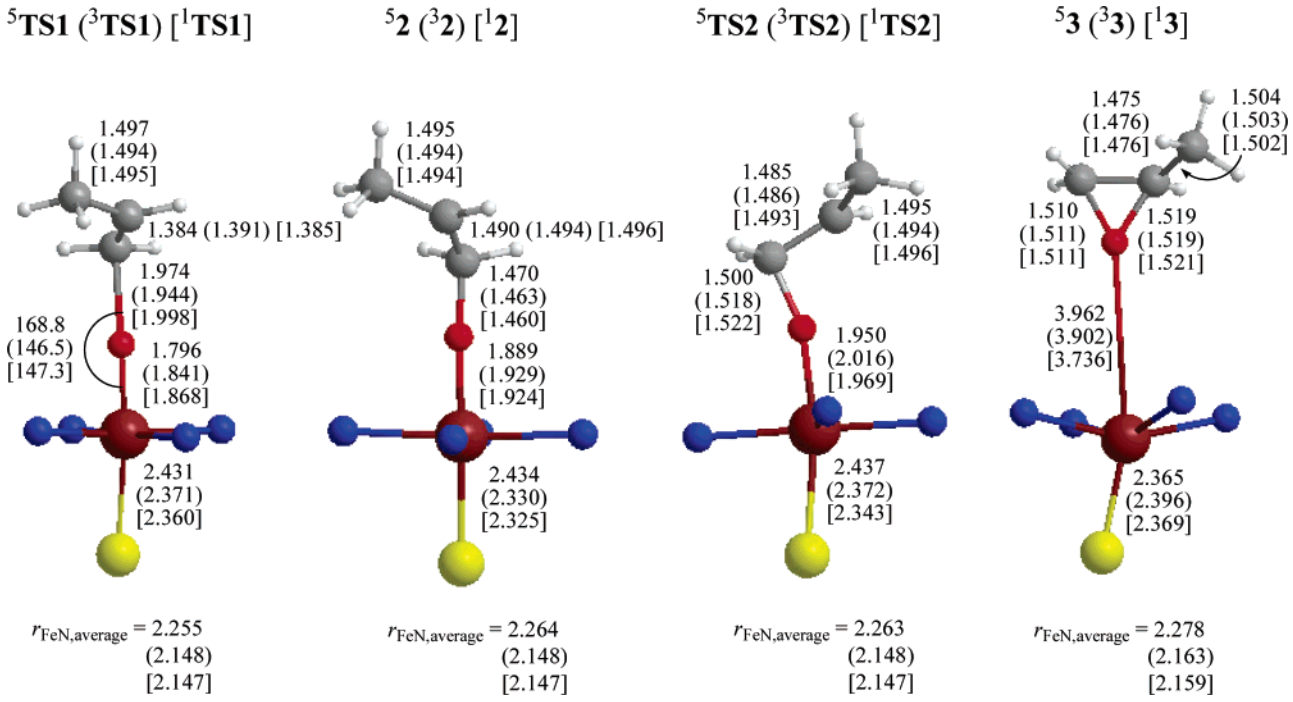

Figure 3. Extracts of optimized geometries of ^{1,3,5}**TS1**, ^{1,3,5}**2**, ^{1,3,5}**TS2**, and ^{1,3,5}**3** for the epoxidation of propene by ^{1,3,5}Fe═O(TMCS)$^+$. All bond lengths are in angstroms, and angles, in degrees.

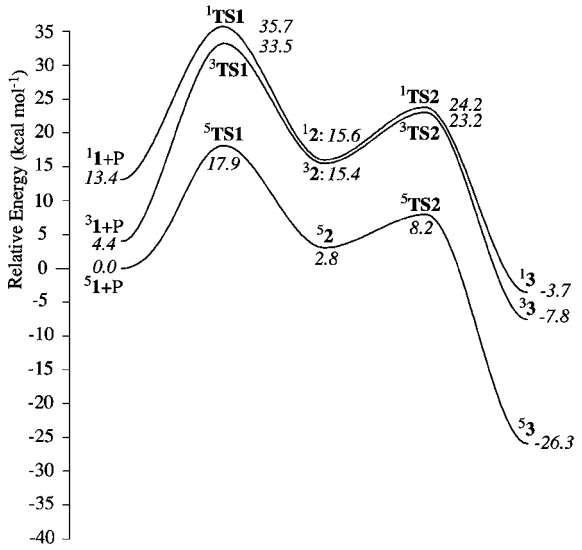

Figure 4. Potential energy profile for the epoxidation reaction of propene by ^{5,3,1}Fe═O(TMCS)$^+$. All energies are in kcal mol^{-1} relative to ^{5}**1** + propene and obtained at the LACV3P+* level of theory with ZPE corrections at the LACVP level.

chemoselectivity of double bond epoxidation vis-à-vis C—H hydroxylation, we calculated the potential energy profile of its reaction with propene (P) leading to propene-oxide and propenol products. The epoxidation reactions occur via a C—O bond formation transition state (**TS1**) leading to a radical intermediate (**2**) that after a ring-closure barrier (**TS2**) is converted into epoxide products (**3**). Figure 3 shows the optimized geometries of the critical points along the reaction pathway, while Figure 4 gives the energy profile for the reaction.

The optimized geometries show much similarity with the ones obtained for propene epoxidation by P450, HRP, and TauD models. In the quintet spin state the substrate attacks the oxo group along the *z*-axis and the Fe—O—C angle is almost linear (168.8°), while in the singlet and triplet spin states the angles are more tilted: 147.3° and 146.5° respectively. Nevertheless, the C—O distances in ^{1,3,5}**TS1** are almost the same. In fact, most bond distances in the singlet, triplet, and quintet spin states are very much alike. In P450 and HRP models the barrier (**TS1**) occurs somewhat earlier with longer C—O distances and shorter Fe—O distances. Approach of the substrate to the oxo group leads to lengthening of the Fe—S bond to 2.431 Å in the quintet spin state due to single occupation of the $\sigma^*_{z^2}$ orbital. This Fe—S distance is almost identical to the one obtained in a P450 model where distances of 2.423 (2.460) Å for ^{4}**TS1** (^{2}**TS1**) were obtained.[18b] Although with Fe═O(TMCS)$^+$ the substrate approaches from the top rather than sideways, most distances are the same as the ones obtained with oxoiron heme models of P450 and HRP.

The initial step from **1** to **2** results in a one electron donation from the substrate into the 3d metal system whereby a radical intermediate (**2**) is formed. In the quintet spin state, similar to the case of TauD, the electron is transferred into the $\sigma^*_{z^2}$ orbital, which is antibonding along the O—Fe—S axis. This weakens the Fe—O bond and pushes the oxygen atom away from the iron center. Moreover, the electron transfer results in a situation whereby the whole 3d block is singly occupied plus a radical on the substrate. This exchange stabilization lowers the quintet spin state in energy. The subsequent ring closure gives another electron transfer into the 3d system filling the $\pi^*_{x^2-y^2}$ orbital with a second electron, thereby reducing the metal to oxidation state Fe^{II}. In oxoiron heme systems the radical on the heme abstracts one electron and the 3d system abstracts another electron, so that the metal is only reduced by one unit in the reaction process from Fe^{IV} to Fe^{III}.

In the triplet spin state, the electron donation to the metal is achieved differently than that in the quintet spin state. Thus, instead of transferring an electron into an empty σ^* orbital, the electron transfer takes place into the singly occupied π^*_{xz} orbital

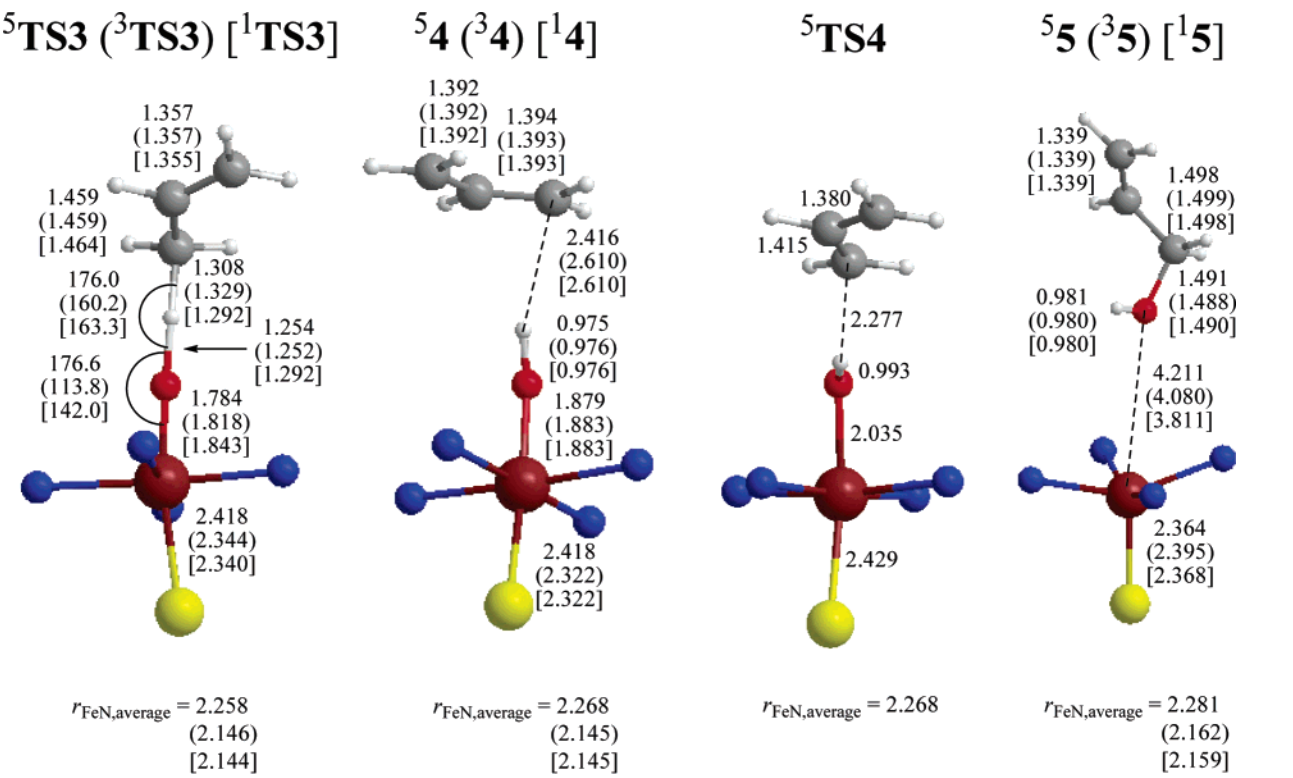

Figure 5. Extracts of optimized geometries of ^{1,3,5}**TS3**, ^{1,3,5}**4**, ^{5}**TS4**, and ^{1,3,5}**5** for the hydroxylation of propene by ^{1,3,5}Fe═O(TMCS)$^{+}$. Bond lengths are in angstroms, and angles, in degrees.

to form an intermediate complex (^{3}**2**) with occupation $\pi^{*}_{x^2-y^2}{}^{2}$ $\pi^{*}_{xz}{}^{2}$ $\pi^{*}_{yz}{}^{1}$. As such, the triplet spin intermediate experiences much less exchange stabilization than the quintet spin intermediate. The singlet and triplet surfaces approach each other closely in the radical intermediate due to the same orbital occupation of $\pi^{*}_{x^2-y^2}{}^{2}$ $\pi^{*}_{xz}{}^{2}$ $\pi^{*}_{yz}{}^{1}$ $\pi_{L}{}^{1}$. The ring-closure step in the triplet spin state leads to an electron transfer into the empty σ^{*}_{xy} orbital.

We also optimized a triplet spin intermediate with $\pi^{*}_{x^2-y^2}{}^{2}$ $\pi^{*}_{xz}{}^{1}$ $\pi^{*}_{yz}{}^{1}$ $\sigma^{*}_{xy}{}^{1}$ $\pi_{L}{}^{1}$ configuration (^{3}**2′**), which is actually lower in energy than ^{3}**2** by 3.2 kcal mol^{-1}. However, this intermediate is connected via a transition state (^{3}**TS1′**) to an excited state of ^{3}**1**, so we did not pursue this mechanism further.

The rate determining step in the gas phase is the initial C—O bond formation barrier **TS1** and is by far the lowest on the quintet spin state surface by 15.6 kcal mol^{-1} over the triplet. Thus, the epoxidation reaction will take place on a dominant quintet spin state surface similar to the reaction performed by a model of TauD. Note as well, the significant ring-closure transition state ^{5}**TS2** of 5.4 kcal mol^{-1}. This implies that ^{5}**2** will have a significant lifetime during which cis−trans isomerizations or other side reactions may take place.

Hydroxylation by Fe═O(TMCS)$^{+}$. We also calculated the hydroxylation of propene by Fe═O(TMCS)$^{+}$. Like the reaction mechanism for the epoxidation reaction it is stepwise via a radical intermediate. The initial step is a hydrogen abstraction barrier (**TS3**) to form a hydroxoiron complexed to an allyl radical (**4**) that rebounds via a rebound transition state (**TS4**) to form the propenol products (**5**). The reaction mechanisms are similar to the ones obtained for TauD and P450 models, where also stepwise mechanisms via radical intermediates were obtained.[17,18] Figure 5 displays the optimized geometries along the hydroxylation pathway, while the potential energy landscape is shown in Figure 6.

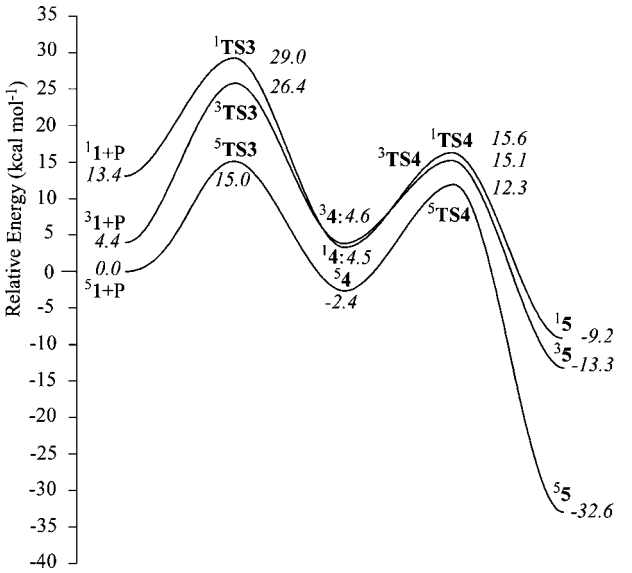

Figure 6. Potential energy profile for the hydroxylation reaction of propene by Fe═O(TMCS)$^{+}$. All energies are in kcal mol^{-1} relative to ^{5}**1** + propene and obtained at the LACV3P+* level of theory with ZPE corrections at the LACVP level.

The optimized geometries in the singlet, triplet, and quintet spin states are very similar, and only minor differences are obtained between the three structures (Figure 5). The substrate attacks the oxo group from the top; hence an almost linear Fe—O—H angle of 176.6° and O—H—C angle of 176.0° are obtained in the quintet spin state. In the quintet and triplet spin states the hydrogen abstraction barrier occurs late with shorter O—H distances than C—H distances, whereas in the singlet spin state the O—H and C—H distances are almost equal. The geometries are very similar to the ones obtained for hydrogen

Table 1. Relative Energies of ^{5,3}**1** and the Rate Determining Transition States ^{5,3}**TS1** and ^{5,3}**TS3** in the Gas Phase, under the Influence of a Dielectric Constant of $\epsilon = 5.7$ and $\epsilon = 10.65$, and with One or Two Hydrogen-Bonded Methanol Molecules (MeOH) Added to the System[a]

state	ΔE + ZPE[b]	+ $E_{\epsilon=5.7}$[c]	+ $E_{\epsilon=10.65}$[c]	+ E_{1MeOH}[d]	+ E_{2MeOH}[e]	+ $E_{1MeOH,opt}$[f]
^{5}**1**	0.0	0.0	0.0	0.0	0.0	0.0
^{3}**1**	4.4	3.1	2.8	4.0	5.1	4.2
^{5}**TS1**	17.9	19.2	19.1	16.7	15.4	17.5
^{5}**TS3**	15.0	16.6	16.7	14.1	12.7	14.5
^{3}**TS1**	33.5	35.1	35.2	33.0	46.4	37.4
^{3}**TS3**	26.4	28.1	28.2	25.9	27.3	26.7

[a] Calculated with UB3LYP/LACV3P+* with ZPE corrections at the LACVP level of theory. [b] In the gas phase. [c] Dielectric constant (ϵ) corrections to the gas-phase ΔE + ZPE values at the LACVP level of theory. [d] One methanol molecule hydrogen-bonded toward sulfur at a fixed distance of 2.3 Å. [e] Two methanol molecules hydrogen-bonded toward sulfur at a fixed distance of 2.3 Å. [f] Fully optimized structure with one hydrogen-bonded methanol molecule in the gas phase.

abstraction of propene by oxoiron systems in P450 and TauD models. Similar to the epoxidation mechanisms discussed above, the only major differences between Fe═O(TMCS)$^+$ on the one hand and the oxoiron species of P450 and TauD on the other hand are the attack of the hydrogen atom from the top and the long Fe—O distance in the product complex here.

The rate determining step in the hydroxylation is the initial hydrogen abstraction barrier with a value of 15.0 kcal mol^{-1} in the gas phase. Similar to the epoxidation reaction, the quintet spin state is well separated from the triplet and singlet spin states by more than 10 kcal mol^{-1}, which means that the quintet spin state will be the dominant pathway. The hydroxylation intermediate, i.e., the hydroxo-iron complex is separated by a relatively large rebound barrier (^{5}**TS4**) of 14.7 kcal mol^{-1}. This long lifetime should enable the system some stereochemical scrambling.

In the triplet spin state we calculated two intermediate structures with orbital occupation $\pi^*_{x^2-y^2}{}^2\ \pi^*_{xz}{}^2\ \pi^*_{yz}{}^1\ \pi_L{}^1$ (^{3}**4**) and $\pi^*_{x^2-y^2}{}^2\ \pi^*_{xz}{}^1\ \pi^*_{yz}{}^1\ \sigma^*_{xy}{}^1\ \pi_L{}^1$ (^{3}**4′**), whereby π_L represents the singly occupied orbital on the allyl group. Although the latter structure is slightly more stable than the former one (by 2.3 kcal mol^{-1}), ^{3}**4′** is connected via a hydrogen abstraction transition state to an excited state of CpdI. Therefore, we did not investigate this alternative mechanism further.

Environmental Effects on Chemoselectivity. As can be seen from Figures 4 and 6, the rate determining steps in the reaction of Fe═O(TMCS)$^+$ with propene are the initial C—O bond formation (via ^{5}**TS1**) in the epoxidation mechanism and the hydrogen abstraction step via ^{5}**TS3** in the hydroxylation reaction. The lowest lying pathway in the gas phase is via ^{5}**TS3**, which is 2.9 kcal mol^{-1} lower in energy than the reaction via ^{5}**TS1** (Table 1). Therefore, in the gas phase Fe═O(TMCS)$^+$ will predominantly react with propene via hydroxylation rather than epoxidation. This is a chemoselectivity reversal with respect to TauD and P450 models, where in the gas phase **TS1** was below **TS3**.[17,18] The absolute barriers of the rate determining steps (^{5}**TS1**, ^{5}**TS3**) are considerably higher in energy than the ones obtained with models of TauD and P450, where barriers of 5.4 (TauD) and 13.0 (P450) kcal mol^{-1} were calculated for **TS3** using the same methods and basis sets.[17,18] Our calculated barriers support experimental studies that showed that only weak C—H hydrogen bonds can be hydroxylated with this catalyst.[3] Since the energy differences between ^{5,3}**1** are small, one would expect a two-state reactivity pattern on competing triplet and quintet spin state surfaces. But, as follows from Figures 4 and 6 above, Fe═O(TMCS)$^+$ reacts via single-state reactivity on a dominant quintet spin state surface in the gas phase. The alternative hydroxylation mechanisms in the triplet and singlet spin states are at least 11.4 and 14.0 kcal mol^{-1} higher in energy and do not play a role of importance.

We have searched for factors that can influence the chemoselectivity of hydroxylation over epoxidation. Initially, we did single-point calculations of the optimized geometries in a dielectric constant (Table 1). As can be seen from Table 1, external perturbations such as a dielectric constant lower the ^{5}**1**—^{3}**1** energy gap, although the quintet spin state stays the ground state under all conditions tested. Addition of a dielectric constant raises the barriers ^{5,3}**TS1** and ^{5,3}**TS3** by 1.2—1.8 kcal mol^{-1} but does not change the ordering of the transition states. Therefore, the effect of a dielectric constant on the chemoselectivity of the reaction is small.

Subsequently, we tested the effect of hydrogen bonding to the thiolate ligand on the spin state ordering and chemoselectivity of the reaction, since it was shown that this can change the charge and spin distributions of oxoiron catalysts with a thiolate axial ligand considerably and as a result even change the chemoselectivity of a reaction.[18b,24] Hydrogen-bonded methanol (MeOH) molecules were added to the sulfur atom of the catalyst, as the experimental work took place in this solvent.[2,3] Initially, we fixed the methanol molecules at a distance of 2.3 Å from the sulfur ligand, but later we reoptimized ^{5,3}**1**, ^{5,3}**TS1**, and ^{5,3}**TS3** with one hydrogen-bonded methanol molecule added to the system. Hydrogen-bonded methanol molecules generally lower the barriers ^{5}**TS1** and ^{5}**TS3** by up to 2.5 kcal mol^{-1}. In particular, with two hydrogen-bonded methanol molecules the lowest barrier (via ^{5}**TS3**) drops to 12.7 kcal mol^{-1}. By contrast, using the same methods and basis sets the barrier ^{2}**TS3** for hydroxylation of propene by Fe═O(Por$^{+\bullet}$)-SH dropped from 13.0 kcal mol^{-1} in the gas phase to 8.9 kcal mol^{-1} with two hydrogen-bonded ammonia molecules.[18ab] Therefore, the effect of external perturbations on the relative energies of the species described in Table 1 is small, and the chemoselective hydroxylation clearly is not the consequence of external perturbations. This is in contrast to Fe═O(Por$^{+\bullet}$)-SH, where the axial ligand was shown to be extremely sensitive to external perturbations due to orbital mixing of the heme a_{2u} orbital with a σ_S sulfur orbital giving the axial ligand some radical character that varied depending on the nature of the external interactions.[18ab,24]

On the triplet spin surface the barriers are only marginally stabilized with one added methanol molecule but destabilized with two hydrogen-bonded methanol molecules. In order to find out whether this had to do with the fact that the geometries were not optimized, we ran full geometry optimizations of ^{5,3}**1**, ^{5,3}**TS1**, and ^{5,3}**TS3** with one hydrogen-bonded methanol molecule added to the system. The optimized geometries of the systems with methanol are labeled ^{5,3}**1**•1MeOH, ^{5,3}**TS1**•1MeOH and ^{5,3}**TS3**•1MeOH, and extracts of their geometries are shown in Figure 7.

A hydrogen-bonded methanol molecule pointing toward the thiolate ligand reduces the Fe—O and elongates the Fe—S distances slightly, cf. Figures 2 and 7, but most other differences are negligible. The charge transfer (Q_{CT}) shown in Figure 7 is

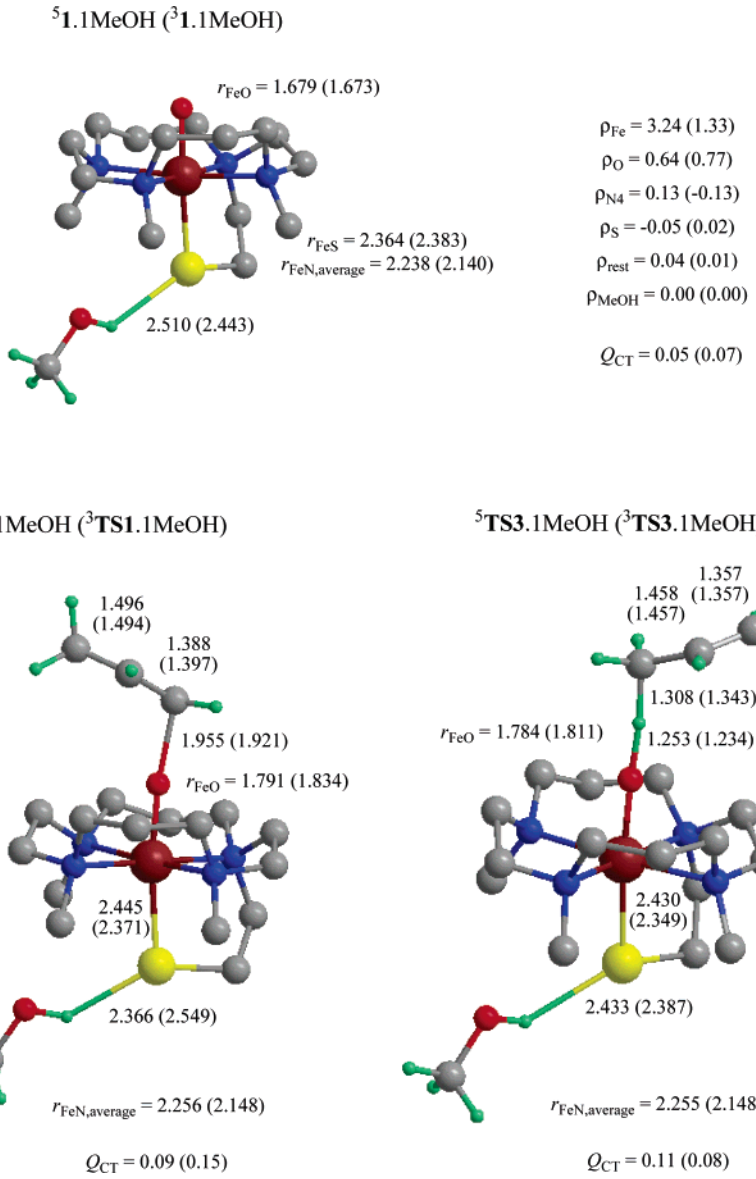

Figure 7. Extracts of optimized geometries of ^{5,3}**1**•1MeOH, ^{5,3}**TS1**•1MeOH, and ^{5,3}**TS3**•1MeOH. The hydrogen atoms of the TMCS ligand have been removed for clarity. All bond lengths are in angstroms, and Q_{CT} is the charge transfer from the sulfur ligand to the methanol molecule. Also shown are group spin densities for ^{5,3}**1**•1MeOH taken from the LACV3P+* results.

the difference in charge of the sulfur atom in the systems with and without methanol. As can be seen values of Q_{CT} between 0.05 and 0.15 are obtained, which implies small charge redistributions within the systems. Although some charge is withdrawn from the thiolate group by the methanol molecule, no significant differences in group spin densities are obtained. In the quintet spin transition states the geometry differences are somewhat larger than those in ^{5}**1**, which is due to the filling of the $\sigma^*_{z^2}$ orbital with one electron. A hydrogen-bonded methanol molecule, however, gives almost the same barrier heights and spin state ordering as the ones obtained in the gas phase without methanol. This implies that the rate constant and substrate catalysis will not be influenced strongly by changes in solvent and the local environment of the catalyst.

Why Does Fe═O(TMCS)$^+$ React via SSR? So what is it that stabilizes the reaction on the quintet spin state surface so much, and why is the hydroxylation pathway favored over the epoxidation reaction? In order to answer these questions, consider first in Figure 8 the electron-transfer processes that happen in the triplet and quintet spin transition states. In the quintet spin state the substrate donates one electron into the metal 3d system, which is used to fill the empty $\sigma^*_{z^2}$ orbital to create an intermediate complex (^{5}**2**, ^{5}**4**) with orbital occupation $\pi^*_{x^2-y^2}{}^1$ $\pi^*_{xz}{}^1$ $\pi^*_{yz}{}^1$ $\sigma^*_{xy}{}^1$ $\sigma^*_{z^2}{}^1$ $\pi_p{}^1$. The latter orbital is the

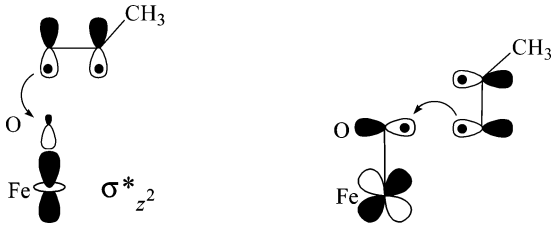

Figure 8. Electron-transfer processes in ^{5}**TS1** and ^{3}**TS1**.

radical on the rest group of propene. Thus, the system gains radical character in this step from four unpaired electrons to six and will be exchange stabilized. Due to electron transfer from the substrate into the $\sigma^*_{z^2}$ orbital, the substrate will be aligned along the molecular *z*-axis. Indeed the geometries shown in Figures 3 and 5 support this, with an Fe—O—C angle of 168.8° (^{5}**TS1**) and an Fe—O—H angle of 176.6° (^{5}**TS3**). By contrast, in the triplet spin state an electron transfer takes place from the substrate into the singly occupied π^*_{xz} orbital, and the substrate tries to align itself sideways. However, electrostatic repulsions of the hydrogen atoms of the TMCS ligand with the substrate prevent an ideal geometry in the triplet state and consequently raises the energies of the triplet barriers well above the quintet barriers. Moreover, the quintet spin pathway is exchange stabilized with six unpaired electrons. Thus, the quintet spin state surface gives efficient monoxygenation activity due to geometric arrangement that follows orbital overlaps and electron-transfer processes. Due to the considerable differences in barrier heights for the rate determining steps on the triplet and quintet spin state surfaces, Fe═O(TMCS)$^+$ will react via single-state reactivity on a dominant quintet spin surface.

Why Does Fe═O(TMCS)$^+$ React via Chemoselective Hydroxylation? Thus, the electron-transfer mechanisms explain why the triplet pathways are much higher in energy than the quintet ones, but it does not distinguish between the epoxidation and hydroxylation mechanisms. The stabilization of the hydroxylation over the epoxidation mechanism follows from the differences in geometries. The rate determining transition states (Figure 9) experience Pauli repulsions between the protons located on the TMCS ligand and the protons on the approaching substrate. This is even more so in ^{5}**TS1** than in ^{5}**TS3**, since the inactive protons of the substrate in ^{5}**TS3** are further away from the TMCS protons than those in ^{5}**TS1** (Figure 9): the nearest proton—proton interaction in ^{5}**TS3** is 2.888 Å, while it is 2.138 Å in ^{5}**TS1**. Therefore, the steric hindrance of the protons on the TMCS ligand with ones on the substrate destabilize the epoxidation mechanism and make the hydroxylation pathway favorable. In heme enzymes, the ligand is almost planar and the substrate is unhindered by side groups of the heme and can approach under ideal circumstances whereby **TS1** is below **TS3**.

Differences in Catalytic Properties of Various Oxoiron Complexes. Table 2 summarizes the differences and comparisons of propene oxidation by various oxoiron complexes as studied with DFT. Two of those, TauD and Fe═O(TMCS)$^+$, are nonheme oxoiron complexes, while the other two are heme-type oxoiron mimics of P450 and HRP enzymes. The latter two systems have an extra oxidation equivalent located on the heme resulting in close lying quartet and doublet spin states of the reactant. These two spin states cause reactions taking place on competing spin state surfaces, i.e., TSR. Generally in heme models, such as P450 and HRP, the two reactant states (doublet and quartet spin) react with substrates via epoxidation and hydroxylation mechanisms with similar barriers. The only exceptions identified until now are arene hydroxylation and sulfoxidation, whereby one of the two spin state surfaces was dominant.[24b,28] Nonheme systems miss the extra oxidation equivalent on the ligand and consequently have the oxoiron species in higher (quintet) spin states. However, Fe═O(TMCS)$^+$ also has a low-lying triplet spin state due to the push effect of the thiolate ligand. Nevertheless, the triplet spin state suffers from high reaction barriers and plays little importance in the reaction, so that both nonheme oxoiron complexes (Table 2) essentially react via SSR.

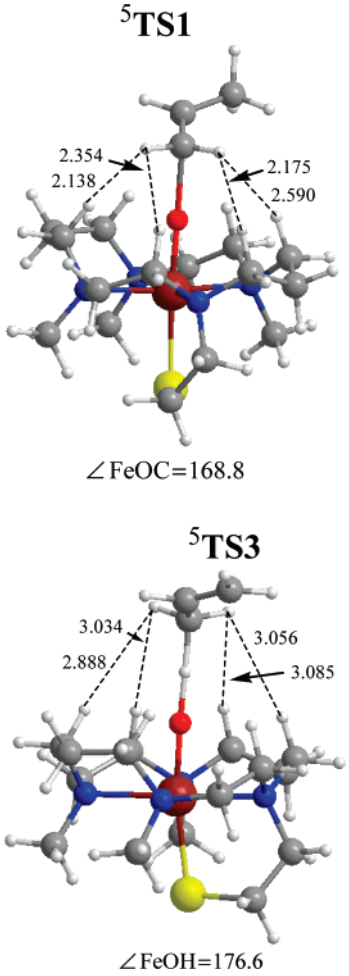

Figure 9. Distances of protons of the TMCS ligand with protons of the substrate for ^{5}**TS1** and ^{5}**TS3**. All distances are in angstroms, and angles, in degrees.

As follows from Table 2, while Fe═O(TMCS)$^+$ prefers chemoselective hydroxylation in the gas phase, all other oxoiron complexes react via chemoselective epoxidation. However, in the case of CpdI of P450, hydrogen bonding and a dielectric constant changed this chemoselectivity in favor of hydroxylation.[18a,b] The catalytic properties of the Fe═O(TMCS)$^+$ system are much less dependent on environmental perturbations than those of the oxoiron species of P450. Yet, the activity of Fe═O(TMCS)$^+$ is not necessarily better than that of the oxoiron heme models, as it is dependent on the population of the quintet spin state of the reactant. As shown above, the triplet and quintet spin states are close in energy, but only the catalysis on the quintet spin state surface is efficient, while the triplet spin state is a sluggish oxidant. In summary, Fe═O(TMCS)$^+$ has similarities with P450 enzymes, such as two close-lying spin states in the reactants and the push effect of the thiolate ligand. However, due to a nonplanar ligand in TMCS the electrostatic interactions of the approaching substrates with the ligands change the reactivity

(28) (a) Sharma, P. K.; de Visser, S. P.; Shaik, S. *J. Am. Chem. Soc.* **2003**, *125*, 8698—8699. (b) Kumar, D.; de Visser, S. P.; Sharma, P. K.; Hirao, H.; Shaik, S. *Biochemistry* **2005**, *44*, 8148—8158.

Table 2. Differences and Comparisons of Reactivity Patterns of Oxoiron Complexes versus Propene[a]

catalyst	heme/nonheme	$2S+1$[a]	SSR/TSR	**TS1**[b,c]	**TS3**[b,c]	reference
Fe═O(TMCS)$^+$	nonheme	5, 3	SSR	17.9	15.0	this work
TauD	nonheme	5	SSR	4.8	5.4	17
P450 CpdI	heme	4, 2	TSR	12.8 (12.3)	14.0 (13.0)	18a,b
HRP CpdI	heme	4, 2	TSR	9.7 (8.5)	10.9 (9.7)	18c

[a] Spin multiplicity. [b] Calculated with UB3LYP/LACV3P+* with ZPE corrections at the LACVP level of theory. [c] The low spin data are in parentheses.

pattern from TSR to SSR, whereby the hydroxylation is stabilized over the epoxidation.

Conclusions

In conclusion, DFT calculations on the reaction of Fe═O(TMCS)$^+$ with propene show that the catalyst predominantly hydroxylates C—H bonds even in the presence of a C═C double bond. This has been analyzed and shown to appear due to lesser stereochemical interactions between the substrate and the TMCS ligand. The push effect of the thiolate ligand brings the triplet and quintet spin states of Fe═O(TMCS)$^+$ close in energy. However, electrostatic repulsions of the protons of the TMCS ligand with atoms of the substrate destabilize the epoxidation barriers considerably and make the hydroxylation process favorable. In summary, Fe═O(TMCS)$^+$ reacts via single-state reactivity (SSR) with chemoselective hydroxylation. This is the first oxoiron complex whereby we find a lower hydroxylation than epoxidation barrier in the gas phase.

Acknowledgment. The National Service of Computational Chemistry Software (NSCCS) is acknowledged for providing CPU time.

Supporting Information Available: Group spin densities and charges of all species calculated for this work under various environmental conditions and using LACVP or LACV3P+* basis sets (12 tables). In addition we show two figures with geometry scans for product formation from intermediate complexes for the epoxidation and hydroxylation mechanisms as well as full ref 23. This material is available free of charge via the Internet at http://pubs.acs.org.

JA065365J